Acta Crystallographica Section A
Foundations and Advances
ISSN 2053-2733

Received 2 April 2013
Accepted 25 August 2013

Symmetry groups of single-wall nanotubes

Ma. Louise Antonette N. De Las Peñas,[a]* Mark L. Loyola,[a] Antonio M. Basilio[b] and Eko Budi Santoso[a]

[a]Mathematics Department, Ateneo de Manila University, Loyola Heights, Quezon City, 1108, Philippines, and [b]Chemistry Department, Ateneo de Manila University, Loyola Heights, Quezon City, 1108, Philippines. Correspondence e-mail: mlp@math.admu.edu.ph

This work investigates the symmetry properties of single-wall carbon nanotubes and their structural analogs, which are nanotubes consisting of different kinds of atoms. The symmetry group of a nanotube is studied by looking at symmetries and color fixing symmetries associated with a coloring of the tiling by hexagons in the Euclidean plane which, when rolled, gives rise to a geometric model of the nanotube. The approach is also applied to nanotubes with non-hexagonal symmetry arising from other isogonal tilings of the plane.

1. Introduction

In the past few years there has been a vast amount of fundamental and applied research on single-wall carbon nanotubes (*e.g.* Iijima & Ichihashi, 1993; Endo *et al.*, 1996; Saito *et al.*, 1998; Damnjanović *et al.*, 1999; Reich *et al.*, 2004). Structural analogs, such as boron nitride (BN), boron carbide (BC_3) and boron carbon nitride (*e.g.* BCN, BC_2N), have also been studied (see, for instance, Chopra *et al.*, 1995; Miyamoto *et al.*, 1994; Liu *et al.*, 1989; Yap, 2009).

In materials research, structural analogs are important in the design of new materials. Analogs of existing molecules and compounds are considered because alteration of some components of the previous material can lead to improvements in some properties. Carbon nanotubes, for instance, are structurally strong, with their electronic properties dependent on their chirality (Dresselhaus *et al.*, 1995). The B–C–N analogs, on the other hand, are expected to maintain the mechanical properties but with variations in other properties, *e.g.* electrical properties. Carbon nanotubes can be conducting or semiconducting while B–C–N nanotubes are insulating (Yap, 2009).

The study of symmetry properties of nanotubes has been relevant for gaining deep insight into their physical (quantum numbers, optical activity, conductivity, among others), electronic, mechanical and magnetic properties which determine their potential applications. Studies on symmetry groups of carbon nanotubes and their structural analogs have been carried out (see Damnjanović *et al.*, 2001; Cotfas, 2006; Barros *et al.*, 2006; Loyola *et al.*, 2012, and references therein). There are also works pertaining to symmetry groups of nanotubes with non-hexagonal symmetry (*e.g.* Milošević & Damnjanović, 2006; Damnjanović *et al.*, 2007; Arezoomand & Taeri, 2009). These tubes, such as those rolled up from two-dimensional rectangular and rhombic lattices, include the incommensurate ones – structures without translational symmetries. Commensurability properties contribute to the physical and electronic characteristics of nanotubes (Milošević & Damnjanović, 2006; Damnjanović *et al.*, 2007; Damnjanović & Milošević, 2010).

In our paper, the objective is to give an alternative approach to determine the symmetry groups of single-wall nanotubes. We use the theory of colorings of tilings in a cylindrical orbit space arising from colored isogonal tilings in the plane as a tool to describe and model single-wall nanotubes and characterize their symmetry properties. Colorings of isogonal tilings are employed as a means to determine different atomic configurations that exist and are theoretically possible for a nanotube.

For carbon nanotubes and their structural analogs, the method involves studying color symmetries associated with a vertex coloring of the tiling by hexagons in the plane which, when folded to form a cylinder, serves as a geometric model for a nanotube. We derive the symmetry group of the nanotube from the color fixing group of the associated coloring of the hexagonal tiling. In addressing nanotubes with non-hexagonal symmetry, we look at color fixing groups associated with their corresponding isogonal tilings on the plane. The color fixing symmetries also shed light on the commensurate properties of the nanotubes.

In our previous study (Loyola *et al.*, 2012), the symmetries of a structural analog of a carbon nanotube are analyzed directly from the three-dimensional symmetries of a given coloring on a cylinder which models the nanotube. On the other hand, in this work, our starting point is to work on colorings of isogonal tilings and to examine the colorings in cylindrical orbit space evolving from these colorings. From this technique, we are able to provide formulas for the color groups and color fixing groups for the colorings in the orbit space using the symmetries of the corresponding planar colorings as basis. The approach offers a convenient way to study symmetries of nanotubes by looking at two-dimensional isometries. It also facilitates the characterization of the line group structure of the symmetry group of the nanotube based

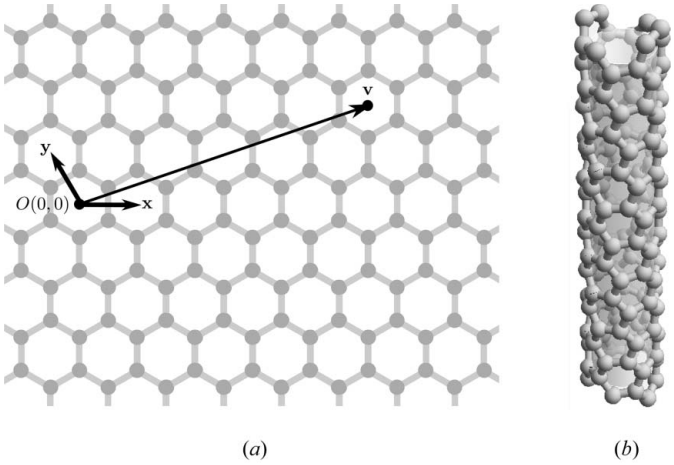

Figure 1
(*a*) The hexagonal tiling together with the translation vectors **x**, **y** and the chiral vector $\mathbf{v} = 6\mathbf{x} + 2\mathbf{y}$. (*b*) The [6, 2] carbon nanotube obtained by rolling up the hexagonal tiling in (*a*) along the chiral vector **v**.

on the plane crystallographic group nature of the symmetry group of the colored tiling in the plane.

Color symmetry theory has been used in the past to describe crystal structures (Harker, 1978; Schwarzenberger, 1984; Senechal, 1988*a*) and quasicrystal/non-periodic structures (Baake, 1997; Lifshitz, 1997; Scheffer & Lück, 1999; Bugarin *et al.*, 2008, 2013). Crystallographers have used colored symmetrical patterns and tilings in several ways, such as in describing arrangements of atoms in a crystal and in deriving magnetic symmetries of crystals and quasiperiodic crystals. This paper highlights the contribution of color symmetry to describe monoperiodic structures, determine atomic arrangements pertaining to nanotube structures and understand their symmetry properties.

The results in this work cover a general class of colorings including *non-perfect colorings* – colorings with color symmetries that form a proper subgroup of the symmetry group of the corresponding uncolored tiling. Modeling nanotubes with atoms that are not equally distributed and studying their symmetry properties require methods in arriving at non-perfect colorings of isogonal tilings and an understanding of how these planar colorings are realized in the cylinder. This study extends and encompasses the ideas on perfect colorings provided in related literature (see, for example, Senechal, 1979, 1988*b*).

The outline of the paper is as follows. In §2, we discuss a geometric model of a single-wall carbon nanotube and the derivation of its symmetry group. §3 presents the setting pertaining to structural analogs of carbon nanotubes. In §4, we outline the concepts in color symmetry theory relevant to the study. The main results on symmetry groups of the structural analogs are given in §5. These results are applied in §6 to derive the symmetry groups of BN, BC_3, BCN and BC_2N nanotubes. In §7, we extend the approach and results of the previous sections to include nanotubes with non-hexagonal symmetry. A short discussion on commensurate and incommensurate nanotubes is included. Finally, in §8, a summary of the paper is presented together with the future outlook of the work.

2. Single-wall carbon nanotubes and their symmetry groups

A geometric model of a single-wall carbon nanotube is constructed by wrapping up a graphene sheet into a seamless cylindrical tube. The graphene sheet is modeled by a tiling $\mathbb{T}$ of the Euclidean plane $\mathbb{E}^2$ by hexagons whose vertices represent carbon atoms and whose edges represent carbon bonds. The sheet (or the hexagonal tiling $\mathbb{T}$) is rolled along a vector **v**, called the *chiral vector* of the tube, emanating from the center of a fixed hexagonal tile, which we assign as the origin $O(0, 0)$, and terminating at the center of another tile so that these centers coincide in the tube (Fig. 1). The vector **v** becomes the circumference of the tube.

The hexagonal tiling $\mathbb{T}$ has symmetry group $G = \langle x, y, a, b\rangle \cong p6mm$ (in IUCr notation) generated by the sixfold (counterclockwise) rotation a about O, the reflection b about the line through O in the direction of **x**, and the translations x, y (Fig. 1*a*). The chiral vector **v** can be expressed as $\mathbf{v} = m\mathbf{x} + n\mathbf{y}$, where $m, n \in \mathbb{Z}$. In which case, we obtain an $[m, n]$ nanotube. If $n = 0$, $m = 0$ or $m = n$, we arrive at a *zigzag* nanotube; if $m = 2n$, $2m = n$ or $m = -n$ we have an *armchair* nanotube. In any other cases, we obtain a *chiral* nanotube. The chiral vectors for the achiral (zigzag and armchair) nanotubes are displayed in Fig. 2(*a*).

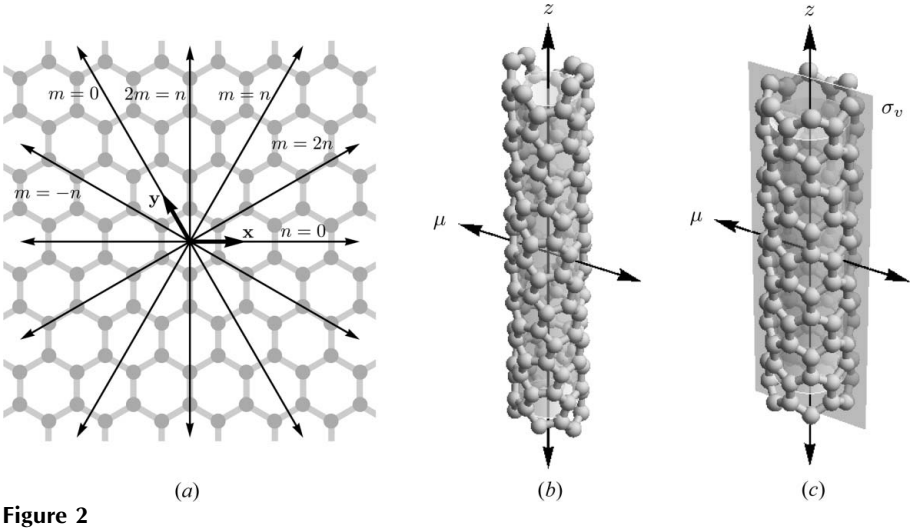

Figure 2
(*a*) Chiral vectors associated with achiral nanotubes. A (*b*) chiral and (*c*) zigzag carbon nanotube, together with the z axis, axis of a twofold rotation μ and mirror plane of the reflection σ_v passing through the z axis.

Let X consist of points in $\mathbb{E}^2$ corresponding to the vertices of the hexagonal tiling $\mathbb{T}$ and let L be a subgroup of the symmetry group G of $\mathbb{T}$ generated

by the translation $l = x^m y^n$, where $m, n \in \mathbb{Z}$. We consider the *orbit space* $L\backslash X = \{Lu : u \in X\}$ of all L-orbits of points in X. Each $v \in X$ belongs to a set $Lu \in L\backslash X$ if and only if v may be obtained from u *via* translation by an integer power of l.

Let us denote by $N_G(L) = \{g \in G : glg^{-1} \in L\}$ the normalizer of L in G. The set of right cosets $N_G(L)\backslash L$ of L in $N_G(L)$ acts on the orbit space $L\backslash X$ by left multiplication. That is, if $Lg \in N_G(L)\backslash L$, $g \in N_G(L)$ and $Lu \in L\backslash X$, then $Lg \cdot Lu = Lgu \in L\backslash X$. It is a well known result from the theory of manifolds (Senechal, 1988*b*; Ratcliffe, 2006) that given the subgroup L (or any torsion-free subgroup) of G, the symmetry group G^* of $L\backslash X$ is isomorphic to $N_G(L)\backslash L$.

In our geometric model of a single-wall carbon nanotube with chiral vector $\mathbf{v} = m\mathbf{x} + n\mathbf{y}$, a point of $L\backslash X$ corresponds to an atom in the nanotube and $G^* \cong N_G(L)\backslash L$ is the symmetry group of the nanotube.

For the chiral $[m, n]$ carbon nanotube with chiral vector $\mathbf{v}_C = m\mathbf{x} + n\mathbf{y}$, we let $L_C = \langle l_C = x^m y^n \rangle$. Among the elements of $G = \langle x, y, a, b \rangle$ that normalize L_C are the twofold rotation a^3 and the translations x and y. We have $N_G(L_C) = \langle x, y, a^3 \rangle \cong p2$. This implies that the symmetry group of the chiral nanotube is $G_C^* \cong N_G(L_C)\backslash L_C \cong (C_d \times \mathbb{Z}) \rtimes C_2$, where $d = gcd(m, n)$. The elements in G_C^* can be described as follows: G_C^* contains the d-fold rotation ρ_d about the z axis brought about by the translation $x^{m/d} y^{n/d}$. Other symmetries in G_C^* include a screw rotation ζ about the z axis brought about by a translation which is neither parallel nor perpendicular to l_C and the twofold rotation μ, which results from the twofold rotation a^3, about an axis passing through the origin and perpendicular to the z axis. We have $G_C^* = \langle \rho_d, \zeta, \mu \rangle$.

The symmetry groups of nanotubes and other monoperiodic structures are also described in terms of *line groups* (Damnjanović *et al.*, 1999, 2001; Damnjanović & Milošević, 2010). These are symmetry groups of structures in Euclidean space $\mathbb{E}^3$ that are periodic only in a single direction (periodicity is assumed to be in the direction of the z axis). There are 13 infinite families of line groups formed by taking products of an infinite cyclic group generated by either a translation, a screw rotation, or a glide reflection, and an axial point group. A complete list of these families and their corresponding group generators is found in Damnjanović *et al.* (2001) and Damnjanović & Milošević (2010). Line groups form an important family of groups which include rod groups, also known as crystallographic line groups (Kopský & Litvin, 2002; Evarestov & Panin, 2012). In the case of the chiral nanotube, its symmetry group G_C^* belongs to line group family 5.

Let us now consider the $[m, 0]$ zigzag carbon nanotube with chiral vector $\mathbf{v}_Z = m\mathbf{x}$ and $L_Z = \langle l_Z = x^m \rangle$. Observe that aside from the twofold rotation a^3, the non-translation elements of G that normalize L_Z include the reflections that are either parallel or perpendicular to l_Z. We thus have $N_G(L_Z) = \langle x, y, a^3, a^3 b \rangle \cong c2mm$ and $G_Z^* \cong N_G(L_Z)\backslash L_Z \cong (C_m \times \mathbb{Z}) \rtimes D_2$. The symmetry group G_Z^* consists of the m-fold rotation ρ_m, a screw rotation ζ' and the twofold rotation μ. As in the chiral nanotube, μ arises from the twofold rotation a^3. The reflection $a^3 b$ about the vertical axis passing through the origin O gives rise to a reflection σ_v with a vertical mirror plane passing through the z axis. The symmetry group of the $[m, 0]$ nanotube is $G_Z^* = \langle \rho_m, \zeta', \mu, \sigma_v \rangle$.

For the $[2n, n]$ armchair carbon nanotube with chiral vector $\mathbf{v}_A = 2n\mathbf{x} + n\mathbf{y}$, we let $L_A = \langle l_A = x^{2n} y^n \rangle$. We obtain similar computations as in the zigzag case, we have $N_G(L_A) = \langle x, y, a^3, a^4 b \rangle \cong c2mm$. The symmetry group G_A^* is generated by the n-fold rotation ρ_n, a screw rotation ζ'', the twofold rotation μ and the reflection σ_v' with a vertical mirror plane passing through the z axis and brought about by the reflection $a^4 b$. That is, $G_A^* \cong N_G(L_A)\backslash L_A \cong (C_n \times \mathbb{Z}) \rtimes D_2$, $G_A^* = \langle \rho_n, \zeta'', \mu, \sigma_v' \rangle$. The symmetry groups of the zigzag and armchair nanotubes belong to line group family 13.

We present in Table 1 a complete list of the symmetry groups of single-wall carbon nanotubes according to chirality. An illustration of a chiral and a zigzag nanotube is given, respectively, in Figs. 2(*b*) and 2(*c*).

Table 1
Symmetry groups of single-wall carbon nanotubes according to chirality.

Chirality		$N_G(L)$	$G^* \cong N_G(L)\backslash L$	Line group
Chiral		$\langle x, y, a^3 \rangle \cong p2$	$(C_d \times \mathbb{Z}) \rtimes C_2$ $d = gcd(m, n)$	5
Zigzag	$n = 0$	$\langle x, y, a^3, a^3 b \rangle \cong c2mm$	$(C_m \times \mathbb{Z}) \rtimes D_2$	13
	$m = n$	$\langle x, y, a^3, a^5 b \rangle \cong c2mm$	$(C_m \times \mathbb{Z}) \rtimes D_2$	13
	$m = 0$	$\langle x, y, a^3, ab \rangle \cong c2mm$	$(C_n \times \mathbb{Z}) \rtimes D_2$	13
Armchair	$m = 2n$	$\langle x, y, a^3, a^4 b \rangle \cong c2mm$	$(C_n \times \mathbb{Z}) \rtimes D_2$	13
	$2m = n$	$\langle x, y, a^3, b \rangle \cong c2mm$	$(C_m \times \mathbb{Z}) \rtimes D_2$	13
	$m = -n$	$\langle x, y, a^3, a^2 b \rangle \cong c2mm$	$(C_m \times \mathbb{Z}) \rtimes D_2$	13

3. Structural analogs of carbon nanotubes

Aside from carbon nanotubes, nanotubes consisting of different types of atoms and having an underlying hexagonal symmetry are of interest in materials research. These are called *structural analogs* of carbon nanotubes. These nanotubes are structurally similar to single-wall carbon nanotubes and can also be described by rolling up the tiling $\mathbb{T}$ by hexagons of the Euclidean plane $\mathbb{E}^2$ into a cylindrical tube. In this case, the vertices of $\mathbb{T}$ represent atoms corresponding to different types of chemical elements. To distinguish an atom from another, we assign different colors to the vertices and we obtain a vertex coloring of $\mathbb{T}$. Rolling up the colored tiling along a vector will give rise to a colored tiling on the cylinder which will represent or model a structural analog of a carbon nanotube.

As an example, let us consider the vertex 3-coloring of the hexagonal tiling $\mathbb{T}$ given in Fig. 3(*a*) with an equal distribution of colors. We roll the colored tiling along the vector $\mathbf{v} = 6\mathbf{x}$ to obtain the colored tiling on the cylinder in Fig. 3(*b*). We arrive at a model of a $[6, 0]$ nanotube made up of an equal distribution of three kinds of atoms, such as a BCN nanotube.

There are other vertex 3-colorings of the hexagonal tiling that give rise to models of BCN nanotubes. See, for example, the colorings presented in Fig. 7. The three colors in the colorings are also equally distributed and suggest other

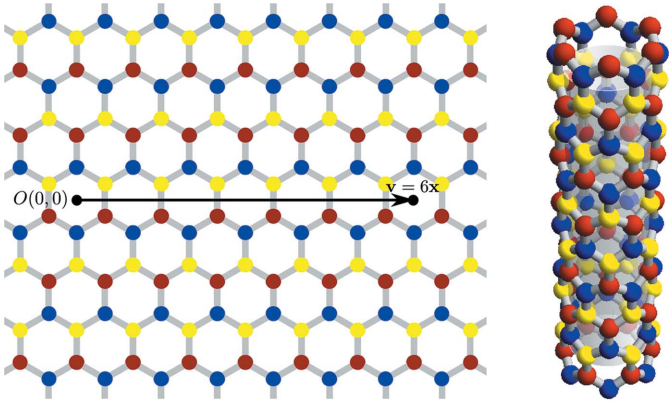

(*a*) (*b*)

Figure 3
(*a*) A vertex coloring of the hexagonal tiling $\mathbb{T}$ with an equal distribution of three colors. (*b*) A 3-coloring of the [6, 0] nanotube representing a BCN nanotube.

arrangements of atoms on a BCN nanotube, distinct from that given in Fig. 3(*a*).

In arriving at vertex colorings of the hexagonal tiling $\mathbb{T}$, our basis is a framework for coloring tilings appearing in De Las Peñas *et al.* (2006, 2011). The framework facilitates a systematic enumeration of vertex k-colorings of a given tiling using the subgroup structure of the symmetry group of the uncolored tiling. The reader can refer to these works for more details on the methodology. In our work, we apply the method hand in hand with GAP (The GAP Group, 2008) and *Mathematica* (Wolfram Research, 2011) to arrive at the colorings. In the next section, we discuss the formalism pertaining to vertex colorings of the hexagonal tiling and the corresponding colorings on the cylinder as well as notions from color symmetry theory that are important points of consideration in determining the symmetry groups of structural analogs of carbon nanotubes.

4. Colorings of single-wall nanotubes and their color symmetries

Let G denote the symmetry group of the uncolored hexagonal tiling $\mathbb{T}$ and X the set of vertices of $\mathbb{T}$. If $C = \{c_1, c_1, \ldots, c_k\}$ is a set of k colors, we define a *vertex* k-coloring of $\mathbb{T}$ to be an onto function $f : X \to C$. Each $u \in X$ is assigned a color in C. The coloring determines a partition $P = \{f^{-1}(c_i) : c_i \in C\}$ where $f^{-1}(c_i)$ is the set of elements of X assigned color c_i.

Let H be the subgroup of G which consists of symmetries in G that effect a permutation of the colors in C. Then $h \in H$ if, for every $c \in C$, there is a $d \in C$ such that $h(f^{-1}(c)) = f^{-1}(d)$. This defines an action of H on C where we write $hc := d$ if and only if $h(f^{-1}(c)) = f^{-1}(d)$. The group H is called the *color group* and the elements of H are referred to as the *color symmetries* of the given coloring of the hexagonal tiling $\mathbb{T}$. The group K of symmetries in H that fix the colors is called the *color fixing group* associated with the coloring. Note that, if $H = G$, then the coloring of $\mathbb{T}$ is called a *perfect coloring*.

Note that, in obtaining a coloring on the cylinder from the colored tiling on the plane, the subgroup $L = \langle x^m y^n \rangle$ of G defining the cylinder or nanotube must be a subgroup of K. This is to ensure that two different colors do not overlap in the cylinder. Given a function $f : X \to C$ that describes a vertex coloring of $\mathbb{T}$, we obtain the onto function $f^* : L\backslash X \to C$ that gives the corresponding coloring on the cylinder.

Let $H^* \leq G^* = N_G(L)\backslash L$ be the color group of the coloring on the cylinder and let $Lg \in H^*$, $g \in N_G(L)$. Then for every $c_i \in C$, there is a $c_j \in C$ such that $(Lg)(f^{*-1}(c_i)) = f^{*-1}(c_j)$ or $(Lg)(c_i) = c_j$. It follows that $gc_i = c_j$. Thus $g \in H$ and $Lg \in N_H(L)\backslash L$. Conversely, if $Lg \in N_H(L)\backslash L$, then we have $Lg \in H^*$. Moreover, if $K^* \leq H^*$ denotes the color fixing group of the coloring on the cylinder, then $Lg \in K^*$ if and only if $Lg \in N_K(L)\backslash L$. Thus, we have the following result.

Theorem. Let H and K denote, respectively, the color group and color fixing group of a vertex coloring of the hexagonal tiling $\mathbb{T}$. Then $H^* = N_H(L)\backslash L$ is the color group and $K^* = N_K(L)\backslash L$ is the color fixing group for the corresponding coloring on the cylinder.

In our study, the main objective is to determine the symmetry properties of a structural analog of a carbon nanotube. In as much as this nanotube is represented by a coloring on the cylinder, our focus is to study the symmetry group of this colored pattern or its color fixing group. From the above theorem, this is given by $K^* \cong N_K(L)\backslash L$. To understand the structure of K^*, a starting point would be to look at the color group $H^* \cong N_H(L)\backslash L$ of the coloring on the cylinder. These ideas are discussed in more detail in the next section.

5. Symmetry groups of structural analogs of carbon nanotubes

Consider a colored cylinder of k colors that models a structural analog of a carbon nanotube consisting of k different atoms. The color group $H^* = N_H(L)\backslash L$ acts on the set C of k colors and, consequently, there exists a homomorphism $\varphi : H^* \to \mathrm{Perm}(C)$, where $\mathrm{Perm}(C)$ is the group of permutations of C. The kernel of φ is $K^* = N_K(L)\backslash L$. Thus, $K^* \trianglelefteq H^*$ or $N_K(L) \trianglelefteq N_H(L)$.

To characterize the structure of $K^* \cong N_K(L)\backslash L$, we use as our basis the two-dimensional symmetries present in $N_K(L)$, $N_K(L) \trianglelefteq N_H(L) \leq N_G(L)$. The planar symmetries in $N_K(L)$ give rise to cylindrical symmetries which define the line group structure of $K^* = N_K(L)\backslash L$. The correspondence between the symmetries is presented in Table 2. In Table 3, we give the line group family structures of K^* with their corresponding generators. The element ζ denotes a screw rotation about the z axis. We have the translation τ with vector parallel to the z axis and a glide reflection γ about a plane passing through the z axis. On the other hand, μ is a twofold rotation about an axis perpendicular to the z axis, while ρ_d is a d-fold rotation about the z axis. Moreover, σ_h is a reflection about a plane perpendicular to the z axis while σ_v is a reflection about a

Table 2
Correspondence between symmetries in $N_K(L)$ and $K^* \cong N_K(L)\backslash L$, $L = \langle x^m y^n \rangle$, $m, n \in \mathbb{Z}$.

Planar symmetries		Cylindrical symmetries
Translation	Parallel to l	Rotation about the z axis
	Perpendicular to l	Translation along the z axis
	Neither parallel, nor perpendicular to l	Screw rotation about the z axis
Twofold rotation		Twofold rotation about an axis perpendicular to the z axis
Reflection	With axis parallel to l	Reflection about a plane perpendicular to the z axis
	With axis perpendicular to l	Reflection about a plane passing through the z axis
Glide reflection	With axis parallel to l	Rotoinversion about the z axis
	With axis perpendicular to l	Glide reflection about a plane passing through the z axis

Table 3
The line group structure of $K^* \cong N_K(L)\backslash L$ based on the plane crystallographic group type of $N_K(L)$.

For families 4, 8, 13, the rotation component of the screw rotation ζ has order $2d$.

$N_K(L)$	Planar symmetries	$K^* \cong N_K(L)\backslash L$ line group family	Line group generators
$p1$		1	ζ, ρ_d
$p2$		5	ζ, ρ_d, μ
cm	Reflection axis parallel to l	4	ζ, ρ_d, σ_h
	Reflection axis perpendicular to l	8	ζ, ρ_d, σ_v
pm	Reflection axis parallel to l	3	τ, ρ_d, σ_h
	Reflection axis perpendicular to l	6	τ, ρ_d, σ_v
$c2mm$		13	$\zeta, \rho_d, \sigma_h, \sigma_v$
$p2mm$		11	$\tau, \rho_d, \sigma_h, \sigma_v$
pg	Glide axis parallel to l	2	τ, λ
	Glide axis perpendicular to l	7	γ, ρ_d
$p2mg$	Glide axis parallel to l	9	τ, λ, σ_v
	Glide axis perpendicular to l	12	$\gamma, \rho_d, \sigma_h, \mu$
$p2gg$		10	γ, λ

plane passing through the z axis. Finally, λ is a $2d$-fold rotoinversion about the z axis.

In the chiral case, for instance, $N_H(L)$ is either of plane crystallographic group type $p1$ or $p2$. This gives rise to two possibilities for $N_K(L)$, $N_K(L) \cong p1$ or $p2$. If $N_K(L) \cong p1$, certain translational symmetries in $N_K(L)$ will result in a screw rotation and a rotation about the z axis in K^*. This implies that K^* belongs to the first family of line groups. If $N_K(L) \cong p2$, aside from the translational symmetries, we have the twofold rotation in $N_K(L)$ that will give rise to a corresponding twofold rotation in K^* about an axis perpendicular to the z axis. Hence, K^* belongs to line group family 5.

For the achiral cases, we consider the following plane crystallographic group types for $N_K(L)$, namely, $p1$, $p2$, cm, pm, $c2mm$, $p2mm$, pg, $p2mg$ and $p2gg$. These are all the possibilities for $N_K(L)$ satisfying $N_K(L) \trianglelefteq N_H(L) \leq N_G(L)$ (Senechal, 1985; Rapanut, 1988).

(i) The first case is when $N_K(L) \cong p1$ or $p2$. Consequently, K^* belongs to line group family 1 or 5, respectively.

(ii) Suppose $N_K(L) \cong cm$ or pm. If $N_K(L) \cong cm$, a translation t, which is neither parallel nor perpendicular to l (Fig. 4*a*), will yield a non-trivial screw rotation in K^*. On the other hand, if $N_K(L) \cong pm$, such a translation (called t' in Fig. 4*b*) will yield a trivial screw rotation in K^*. (A screw rotation in K^* is referred to as trivial if its rotation and translation components are also symmetries in K^*.)

To characterize K^* further, we consider the reflections in $N_K(L)$. If $N_K(L) \cong cm$ or pm, then it contains reflections in one direction. If the axes of reflections are parallel to l, then we obtain a reflection about a plane perpendicular to the z axis. In this case, K^* belongs to line group family 4 if $N_K(L) \cong cm$, or to line group family 3 if $N_K(L) \cong pm$. On the other hand, if the axes of reflections are perpendicular to l, then there is a reflection about a plane passing through the z axis. We obtain K^* to be of line group family 8 if $N_K(L) \cong cm$, or of line group family 6 if $N_K(L) \cong pm$.

(iii) If $N_K(L) \cong c2mm$ or $p2mm$, then $N_K(L)$ contains reflections in two directions. Consequently, we obtain a reflection about a plane perpendicular to the z axis as well as a reflection about a plane passing through the z axis. If $N_K(L) \cong c2mm$, we have a similar case as $N_K(L) \cong cm$, where there is a translation that will yield a non-trivial screw rotation, implying that K^* belongs to line group family 13. On the other hand, if $N_K(L) \cong p2mm$, then K^* belongs to line group family 11.

(iv) If $N_K(L) \cong pg$, then $N_K(L)$ contains glide reflections in one direction and no reflections. If a glide reflection axis is parallel to l, we get a rotoinversion about the z axis and thus K^* belongs to line group family 2. On the other hand, if a glide reflection axis is perpendicular to l, we get a glide reflection about a plane passing through the z axis. In this case, K^* belongs to line group family 7.

(v) If $N_K(L) \cong p2mg$, then $N_K(L)$ contains glide reflections and reflections. As in (iv), if the glide reflection axis is parallel to l, we get a rotoinversion about the z axis. In this case, the reflection has an axis perpendicular to l, so we also obtain a reflection about a plane passing through the z axis. Thus, K^* belongs to line group family 9. On the other hand, if the glide reflection axis is perpendicular to l, we get a glide reflection

Figure 4
Respective translations t and t' on the lattice corresponding to (*a*) $N_K(L) \cong cm$ and (*b*) $N_K(L) \cong pm$.

Table 4
The restrictions on the values of m, n for the chiral vector $\mathbf{v} = m\mathbf{x} + n\mathbf{y}$ in arriving at nanotubes from the colorings shown in Figs. 6, 7 and 8.

$B_xC_yN_z$	Figure	Restriction
BC_3	Fig. 6 (*a*)	$m, n \in 2\mathbb{Z}$
	(*b*)	$n \in 2\mathbb{Z}$
	(*c*)	$2m - n \in 4\mathbb{Z}, n \in 2\mathbb{Z}$
BCN	Fig. 7 (*a*)	$2m - n \in 6\mathbb{Z}, n \in 2\mathbb{Z}$
	(*b*)	$4m + n \in 12\mathbb{Z}, n \in 4\mathbb{Z}$
BC_2N	Fig. 8 (*a*)	$m \in 2\mathbb{Z}$
	(*b*)	$m, n \in 2\mathbb{Z}$
	(*c*)	$n \in 2\mathbb{Z}$
	(*d*)	$n \in 4\mathbb{Z}$
	(*e*)	$2m - n \in 4\mathbb{Z}, n \in 2\mathbb{Z}$
	(*f*)	$n \in 2\mathbb{Z}$
	(*g*)	$n \in 4\mathbb{Z}$
	(*h*)	$m \in 2\mathbb{Z}, n \in 4\mathbb{Z}$
	(*i*)	$m + n \in 4\mathbb{Z}$
	(*j*)	$m + n \in 8\mathbb{Z}, m - n \in 2\mathbb{Z}$
	(*k*)	$m + n \in 4\mathbb{Z}$
	(*l*)	$m + n \in 4\mathbb{Z}$

about a plane passing through the z axis and a reflection about a plane perpendicular to the z axis. Thus, K^* belongs to line group family 12.

(vi) Lastly, if $N_K(L) \cong p2gg$, then $N_K(L)$ contains glide reflections in two directions and no reflections. In this case, since the glide reflections in $N_K(L)$ have axes which are both parallel and perpendicular to l, then K^* contains a rotoinversion about the z axis together with a glide reflection about a plane passing through the z axis. Hence K^* possesses line group family 10 symmetries.

We give a summary of the discussion above in Table 3.

If we consider the coloring in Fig. 3(*a*), which gives rise to a BCN nanotube, we find that its color fixing group is $K = \langle x, y^3, a^3b\rangle \cong cm$. Now, depending on the chiral vector of the nanotube, we get different plane crystallographic group structures for $N_K(L)$. For instance, in the chiral case, when $L = \langle x^m y^n\rangle$, $N_G(L) = \langle a^3, x, y\rangle \cong p2$, we obtain $N_K(L) = K \cap N_G(L) = \langle x, y^3\rangle \cong p1$. From the result given in Table 3, K^* belongs to line group family 1. For the zigzag nanotube with $L = \langle x^m\rangle$, $N_K(L) = \langle x, y^3, a^3b\rangle \cong cm$, we find that the axis of reflection a^3b is perpendicular to the chiral vector $m\mathbf{x}$. Hence, the symmetries of K^* belong to line group family 8. On the other hand, for the armchair nanotube with $L = \langle x^m y^{2m}\rangle$, $N_K(L) = \langle x, y^3, a^3b\rangle \cong cm$. But this time, the axis of reflection a^3b is parallel to the chiral vector $m\mathbf{x} + 2m\mathbf{y}$. Thus, K^* belongs to line group family 4. For the other achiral nanotubes, $N_K(L) = \langle x, y^3\rangle \cong p1$, so K^* belongs to line group family 1. Hence, for a BCN nanotube obtained from the 3-coloring in Fig. 3(*a*), the symmetry group belongs to line group family 1, 4 or 8 depending on the chirality.

6. Symmetry groups of BN, BCN, BC_3 and BC_2N nanotubes

In this part of the paper, we apply the results given in the previous section to derive the symmetry groups of particular structural analogs of a carbon nanotube, such as BN, BC_3, BCN and BC_2N nanotubes.

Note that the restrictions on the values of m, n for the chiral vector $\mathbf{v} = m\mathbf{x} + n\mathbf{y}$ in order to arrive at BC_3, BCN and BC_2N nanotubes are presented in Table 4.

Table 5
Line group symmetry structure of nanotubes arising from the coloring given in Fig. 5.

Chirality		$N_K(L)$	Line group K^*
Chiral		$\langle x, y\rangle \cong p1$	1
Zigzag	$n = 0$	$\langle x, y, a^3b\rangle \cong cm$	8
	$m = n$	$\langle x, y, a^5b\rangle \cong cm$	8
	$m = 0$	$\langle x, y, ab\rangle \cong cm$	8
Armchair	$m = 2n$	$\langle x, y, ab\rangle \cong cm$	4
	$2m = n$	$\langle x, y, a^3b\rangle \cong cm$	4
	$m = -n$	$\langle x, y, a^5b\rangle \cong cm$	4

6.1. BN nanotubes

The vertex 2-coloring of the hexagonal tiling given in Fig. 5, when folded along a chiral vector, will result in a model of a BN nanotube. The vertices of the hexagonal tiling are assigned two colors, which are equally distributed, to represent the boron and nitrogen atoms. The color fixing group of the coloring is given by $K = \langle x, y, a^2, ab\rangle \cong p3m1$. Depending on the chirality of the nanotube, we calculate $N_K(L)$ and determine its plane crystallographic group type. We arrive at the line group structure of $K^* = N_K(L)\backslash L$ presented in Table 5. For a chiral nanotube, $N_K(L) \cong p1$ and K^* belongs to line group family 1. For the zigzag nanotubes, $N_K(L) \cong cm$. The axes of the reflections in $N_K(L)$ are perpendicular to l. Thus, K^* belongs to line group family 8. For the armchair nanotubes, $N_K(L)$ is also of type cm. However, the axes of reflections in $N_K(L)$ are parallel to l. In this case, K^* belongs to line group family 4.

Note that the coloring on the cylinder obtained from the 2-coloring presented in Fig. 5 can also serve as a model for other structural analogs of carbon nanotubes, such as gallium nitride (GaN) and aluminium nitride (AlN) nanotubes. These analogs also possess an equal distribution of two atoms. Our calculations suggest that these nanotubes also have the same symmetry groups as the BN nanotubes. The same symmetry group structure of BN and GaN nanotubes has been reported

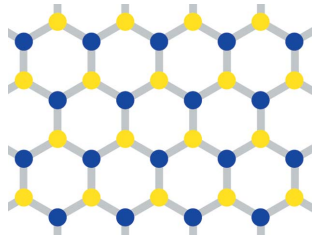

Figure 5
A vertex 2-coloring of the hexagonal tiling that gives rise to a BN nanotube.

Table 6
Line group symmetry structure of BC_3 nanotubes arising from the colorings given in Fig. 6.

Chirality		Fig. 6(*a*)		Fig. 6(*b*)		Fig. 6(*c*)	
		$N_K(L)$	Line group K^*	$N_K(L)$	Line group K^*	$N_K(L)$	Line group K^*
Chiral		$\langle x^2, y^2, a^3\rangle \cong p2$	5	$\langle x, y^2\rangle \cong p1$	1	$\langle x^2, xy^2, xa^3\rangle \cong p2$	5
Zigzag	$n = 0$	$\langle x^2, y^2, a^3b, b\rangle \cong c2mm$	13	$\langle x, y^2, a^3b\rangle \cong pm$	6	$\langle x^2, xy^2, xb, a^3b\rangle \cong p2mg$	9
	$m = n$	$\langle x^2, y^2, a^2b, a^5b\rangle \cong c2mm$	13	$\langle x, y^2\rangle \cong p1$	1	$\langle x^2, xy^2, xa^3\rangle \cong p2$	5
	$m = 0$	$\langle x^2, y^2, ab, a^4b\rangle \cong c2mm$	13	$\langle x, y^2\rangle \cong p1$	1	$\langle x^2, xy^2, xa^3\rangle \cong p2$	5
Armchair	$m = 2n$	$\langle x^2, y^2, ab, a^4b\rangle \cong c2mm$	13	$\langle x, y^2\rangle \cong p1$	1	$\langle x^2, xy^2, xa^3\rangle \cong p2$	5
	$2m = n$	$\langle x^2, y^2, a^3b, b\rangle \cong c2mm$	13	$\langle x, y^2, a^3b\rangle \cong pm$	3	$\langle x^2, xy^2, xb, a^3b\rangle \cong p2mg$	12
	$m = -n$	$\langle x^2, y^2, a^2b, a^5b\rangle \cong c2mm$	13	$\langle x, y^2\rangle \cong p1$	1	$\langle x^2, xy^2, xa^3\rangle \cong p2$	5

in Damnjanović *et al.* (2001), Alon (2001) and Evarestov *et al.* (2010).

6.2. BC_3 nanotubes

In obtaining geometric models for BC_3 nanotubes, we construct vertex 2-colorings of the hexagonal tiling using two colors that appear in the ratio of 3:1, as shown in Fig. 6. The red and yellow colors represent carbon and boron, respectively. The symmetry groups of the BC_3 nanotubes arising from the colorings given in Fig. 6 are summarized in Table 6. The symmetry groups of the BC_3 nanotube arising from the coloring given in Fig. 6(*a*) are also reported in Damnjanović *et al.* (2001). The symmetric arrangements of the boron and carbon atoms appearing in Figs. 6(*b*) and 6(*c*), which suggest other atomic configurations of a BC_3 nanotube, appear in Wang *et al.* (1996) and Azevedo & de Paiva (2006).

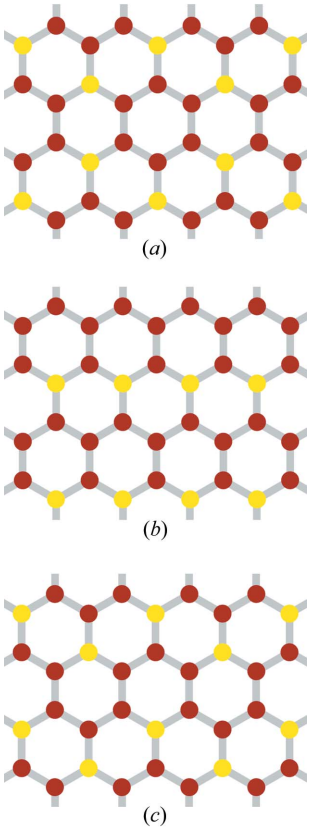

Figure 6
Vertex 2-colorings of the hexagonal tiling that give rise to BC_3 nanotubes. (*a*) $K = \langle x^2, y^2, a, b\rangle \cong p6mm$, (*b*) $K = \langle x, y^2, a^3b\rangle \cong pm$, (*c*) $K = \langle x^2, xy^2, xb, a^3b\rangle \cong p2mg$.

6.3. BCN nanotubes

As discussed previously, a model for a BCN nanotube will arise by considering vertex 3-colorings of the hexagonal tiling with an equal distribution of three colors. We present in Fig. 7 two other 3-colorings that will give rise to BCN nanotubes. The atomic configurations suggested by these colorings are among the most stable carbon–boron–nitride ternary graphite-like monolayers as reported in Azevedo & de Paiva (2006). The symmetry groups of the corresponding BCN nanotubes are given in Table 7.

6.4. BC_2N nanotubes

In this part of the paper, we enumerate various 3-colorings of the hexagonal tiling associated with BC_2N nanotubes and present their corresponding symmetry groups. The colors we use in the colorings are yellow, red and blue that appear in the ratio of 1:2:1. They are used to represent boron, carbon and nitrogen, respectively. We adopt the methodology given in De Las Peñas *et al.* (2006, 2011) and obtained each coloring by specifying a color group H which is a subgroup of the symmetry group $G = \langle a, b, x, y\rangle \cong p6mm$ of the hexagonal tiling. Eliminating the colorings with adjacent boron and nitrogen atoms, we arrive at the colorings presented in Fig. 8. In constructing these colorings, we consider H such that $[G : H] \leq 20$. In these examples, the set of vertices of the tiling form two equal orbits under H. The symmetry groups for the resulting BC_2N nanotubes are presented in Table 8. Results indicate that we have line group families 5 and 13 for the BC_2N (type I) nanotubes and line group families 1, 3 and 6 for the BC_2N (type II) nanotubes (refer to Damnjanović *et al.*, 2001 and Pan *et al.*, 2009 for comparison). For the BC_2N (type III) nanotubes (Liu *et al.*, 1989), we also obtain line group families 1, 3 and 6. Our calculations suggest other types of nanotubes other than those of types I, II and III.

Table 7
Line group symmetry structure of BCN nanotubes arising from the colorings given in Fig. 7.

Chirality		Fig. 7(*a*)		Fig. 7(*b*)	
		$N_K(L)$	Line group K^*	$N_K(L)$	Line group K^*
Chiral		$\langle x^3, xy^2\rangle \cong p1$	1	$\langle x^3, xy^{-4}\rangle \cong p1$	1
Zigzag	$n = 0$	$\langle x^3, xy^2, a^3b\rangle \cong pm$	6	$\langle x^3, xy^{-4}, a^3b\rangle \cong pm$	6
	$m = n$	$\langle x^3, xy^2\rangle \cong p1$	1	$\langle x^3, xy^{-4}\rangle \cong p1$	1
	$m = 0$	$\langle x^3, xy^2\rangle \cong p1$	1	$\langle x^3, xy^{-4}\rangle \cong p1$	1
Armchair	$m = 2n$	$\langle x^3, xy^2\rangle \cong p1$	1	$\langle x^3, xy^{-4}\rangle \cong p1$	1
	$2m = n$	$\langle x^3, xy^2, a^3b\rangle \cong pm$	3	$\langle x^3, xy^{-4}, a^3b\rangle \cong pm$	3
	$m = -n$	$\langle x^3, xy^2\rangle \cong p1$	1	$\langle x^3, xy^{-4}\rangle \cong p1$	1

7. Nanotubes with non-hexagonal symmetry

The approach discussed in the previous sections to determine symmetry groups of carbon nanotubes and their structural analogs can be adapted to a more general setting, when the tubes may not necessarily have hexagonal symmetry.

Synonymous to a graphene sheet, a monolayer consisting of a single type of atom may be modeled geometrically using an isogonal tiling $\mathbb{S}$ of $\mathbb{E}^2$. Isogonal tilings are vertex-transitive and include, among others, the 11 Archimedean tilings and the tilings whose faces are the unit cells of the five two-dimensional Bravais lattices (Grünbaum & Shephard, 1978). In the model, vertices of $\mathbb{S}$ represent atoms and edges represent bonds. Just like a carbon nanotube, a cylindrical tube is obtained by wrapping up the monolayer of atoms (or the tiling $\mathbb{S}$) along a chiral vector $\mathbf{v}$. If x, y with vectors $\mathbf{x}$, $\mathbf{y}$ are the generating translational symmetries of the symmetry group G of $\mathbb{S}$, then the chiral vector of the nanotube can be expressed as $\mathbf{v} = m\mathbf{x} + n\mathbf{y}$, where $m, n \in \mathbb{Z}$, and we obtain an $[m, n]$ single-wall nanotube. Employing the orbit space approach discussed in §2, the resulting nanotube has symmetry group $G^* \cong N_G(L)\backslash L$, where L is the subgroup of G generated by the translation with vector $\mathbf{v}$.

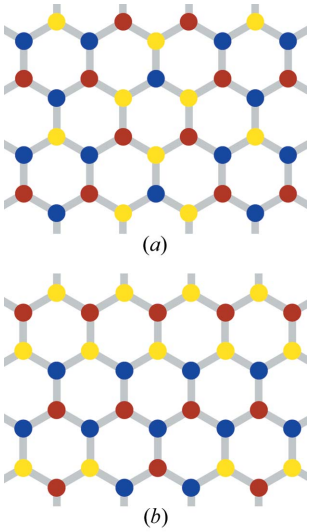

Figure 7
Vertex 3-colorings of the hexagonal tiling that give rise to BCN nanotubes. (*a*) $K = \langle x^3, xy^2, a^3b\rangle \cong pm$, (*b*) $K = \langle x^3, xy^{-4}, a^3b\rangle \cong pm$.

To illustrate these ideas, we consider a nanotube rolled up from a monolayer made up of carbon atoms located at the vertices of a $4 \cdot 8^2$ tiling shown in Fig. 9(*a*). This isogonal tiling has faces consisting of regular octagons and squares. Its symmetry group is given by $G = \langle x, y, a, b\rangle \cong p4mm$ generated by the fourfold (counterclockwise) rotation a about O, the reflection b about the line through O in the direction of $\mathbf{x}$, and the translations x, y. If we fold this $4 \cdot 8^2$ tiling along the chiral vector $\mathbf{v} = m\mathbf{x} + n\mathbf{y}$, which determines the subgroup $L = \langle x^m y^n\rangle$, we obtain an $[m, n]$ TUC_4C_8 nanotube (Arezoomand & Taeri, 2009; Heydari & Taeri, 2009). For example, a $[4, 0]$ TUC_4C_8 nanotube is presented in Fig. 9(*b*).

We compute the symmetry group $G^* \cong N_G(L)\backslash L$ of the TUC_4C_8 nanotube and determine its line group structure. The computations based on chirality are given in Table 9. The results indicate that in addition to line group families 5 and 13, to which the symmetry group of a single-wall carbon nanotube belongs, the symmetry group of a TUC_4C_8 nanotube may also belong to line group family 11. The results we obtain are consistent with the symmetry groups of the TUC_4C_8 nanotubes computed by Arezoomand & Taeri (2009).

Now, in obtaining nanotubes consisting of k different atoms, we consider a k-vertex coloring of $\mathbb{S}$. To ensure that no two types of atoms or colors coincide in the tube, the subgroup L determined by the tube's chiral vector must be a subgroup of the color fixing group K of the coloring. The symmetry group of the nanotube is given by $K^* \cong N_K(L)\backslash L$.

In analyzing the two-dimensional symmetries present in $N_K(L)$, we remark that if a symmetry $g \in K$ normalizes the subgroup L (whose non-identity elements consist of translations), then g must send an element of L to itself or to its inverse. It follows that g cannot be a rotation of order greater than 2. Hence, the possible plane crystallographic group types for $N_K(L)$ are $p1$, $p2$, cm, pm, $c2mm$, $p2mm$, pg, $p2mg$ and $p2gg$. As mentioned in §5, this list includes all the possible crystallographic types for $N_K(L)$ satisfying $N_K(L) \trianglelefteq N_H(L) \leq N_G(L)$, where H is the color group of the colored tiling. Thus, Table 3 gives a complete characterization of all the possible line group structures of nanotubes rolled up from colored isogonal tilings with a crystallographic color fixing group.

We show in Fig. 10(*a*) a vertex 3-coloring of the $4 \cdot 8^2$ tiling. Its color fixing group is given by $K = \langle x, y, a^2b\rangle \cong pm$. The colored tiling is rolled along the vector $\mathbf{v} = 4\mathbf{x}$ to obtain the

Table 8
Line group symmetry structures of BC_2N nanotubes arising from the colorings given in Fig. 8.

Chirality		Fig. 8(*a*) $N_K(L)$	Line group K^*	Fig. 8(*b*) $N_K(L)$	Line group K^*	Fig. 8(*c*) $N_K(L)$	Line group K^*	Fig. 8(*d*) $N_K(L)$	Line group K^*
Chiral		$\langle x^2, y\rangle$ *p*1	1	$\langle x^2, y^2, a^3\rangle$ *p*2	5	$\langle x, y^2\rangle$ *p*1	1	$\langle x, y^4, a^3\rangle$ *p*2	5
Zigzag	$n = 0$	$\langle x^2, y\rangle$ *p*1	1	$\langle x^2, y^2, a^3b, b\rangle$ *c*2*mm*	13	$\langle x, y^2, a^3b\rangle$ *pm*	6	$\langle x, y^4, a^3b, b\rangle$ *p*2*mm*	11
	$m = n$	$\langle x^2, y\rangle$ *p*1	1	$\langle x^2, y^2, a^3\rangle$ *p*2	5	$\langle x, y^2\rangle$ *p*1	1	$\langle x, y^4, a^3\rangle$ *p*2	5
	$m = 0$	$\langle x^2, y, ab\rangle$ *pm*	6	$\langle x^2, y^2, a^3\rangle$ *p*2	5	$\langle x, y^2\rangle$ *p*1	1	$\langle x, y^4, a^3\rangle$ *p*2	5
Armchair	$m = 2n$	$\langle x^2, y, ab\rangle$ *pm*	3	$\langle x^2, y^2, a^3\rangle$ *p*2	5	$\langle x, y^2\rangle$ *p*1	1	$\langle x, y^4, a^3\rangle$ *p*2	5
	$2m = n$	$\langle x^2, y\rangle$ *p*1	1	$\langle x^2, y^2, a^3b, b\rangle$ *c*2*mm*	13	$\langle x, y^2, a^3b\rangle$ *pm*	3	$\langle x, y^4, a^3b, b\rangle$ *p*2*mm*	11
	$m = -n$	$\langle x^2, y\rangle$ *p*1	1	$\langle x^2, y^2, a^3\rangle$ *p*2	5	$\langle x, y^2\rangle$ *p*1	1	$\langle x, y^4, a^3\rangle$ *p*2	5

Chirality		Fig. 8(*e*) $N_K(L)$	Line group K^*	Fig. 8(*f*) $N_K(L)$	Line group K^*	Fig. 8(*g*) $N_K(L)$	Line group K^*	Fig. 8(*h*) $N_K(L)$	Line group K^*
Chiral		$\langle x^2, xy^2, xa^3\rangle$ *p*2	5	$\langle x, y^2\rangle$ *p*1	1	$\langle x, y^4, ya^3\rangle$ *p*2	5	$\langle x^2, y^4\rangle$ *p*1	1
Zigzag	$n = 0$	$\langle x^2, xy^2, xa^3, a^3b\rangle$ *p*2*mg*	9	$\langle x, y^2, a^3b\rangle$ *pm*	6	$\langle x, y^4, ya^3, a^3b\rangle$ *p*2*mg*	9	$\langle x^2, y^4, ya^3b\rangle$ *pg*	7
	$m = n$	$\langle x^2, xy^2, xa^3\rangle$ *p*2	5	$\langle x, y^2\rangle$ *p*1	1	$\langle x, y^4, ya^3\rangle$ *p*2	5	$\langle x^2, y^4\rangle$ *p*1	1
	$m = 0$	$\langle x^2, xy^2, xa^3\rangle$ *p*2	5	$\langle x, y^2\rangle$ *p*1	1	$\langle x, y^4, ya^3\rangle$ *p*2	5	$\langle x^2, y^4\rangle$ *p*1	1
Armchair	$m = 2n$	$\langle x^2, xy^2, xa^3\rangle$ *p*2	5	$\langle x, y^2\rangle$ *p*1	1	$\langle x, y^4, ya^3\rangle$ *p*2	5	$\langle x^2, y^4\rangle$ *p*1	1
	$2m = n$	$\langle x^2, xy^2, xa^3, a^3b\rangle$ *p*2*mg*	12	$\langle x, y^2, a^3b\rangle$ *pm*	3	$\langle x, y^4, ya^3, a^3b\rangle$ *p*2*mg*	12	$\langle x^2, y^4, ya^3b\rangle$ *pg*	2
	$m = -n$	$\langle x^2, xy^2, xa^3\rangle$ *p*2	5	$\langle x, y^2\rangle$ *p*1	1	$\langle x, y^4, ya^3\rangle$ *p*2	5	$\langle x^2, y^4\rangle$ *p*1	1

Chirality		Fig. 8(*i*) $N_K(L)$	Line group K^*	Fig. 8(*j*) $N_K(L)$	Line group K^*	Fig. 8(*k*) $N_K(L)$	Line group K^*	Fig. 8(*l*) $N_K(L)$	Line group K^*
Chiral		$\langle x^4, xy^{-1}\rangle$ *p*1	1	$\langle xy^{-1}, a^3x^{-1}\rangle$ *p*2	5	$\langle x^4, xy^{-1}\rangle$ *p*1	1	$\langle x^4, xy^{-1}\rangle$ *p*1	1
Zigzag	$n = 0$	$\langle x^4, xy^{-1}\rangle$ *p*1	1	$\langle xy^{-1}, xa^3\rangle$ *p*2	5	$\langle x^4, xy^{-1}\rangle$ *p*1	1	$\langle x^4, xy^{-1}\rangle$ *p*1	1
	$m = n$	$\langle x^4, xy^{-1}, xa^5b\rangle$ *pg*	7	$\langle xy^{-1}, xa^3, a^5y^{-1}bx\rangle$ *p*2*gg*	10	$\langle x^4, xy^{-1}, xa^5b\rangle$ *pg*	7	$\langle x^4, xy^{-1}, axab\rangle$ *pg*	2
	$m = 0$	$\langle x^4, xy^{-1}\rangle$ *p*1	1	$\langle xy^{-1}, xa^3\rangle$ *p*2	5	$\langle x^4, xy^{-1}\rangle$ *p*1	1	$\langle x^4, xy^{-1}\rangle$ *p*1	1
Armchair	$m = 2n$	$\langle x^4, xy^{-1}\rangle$ *p*1	1	$\langle xy^{-1}, xa^3\rangle$ *p*2	5	$\langle x^4, xy^{-1}\rangle$ *p*1	1	$\langle x^4, xy^{-1}\rangle$ *p* 1	1
	$2m = n$	$\langle x^4, xy^{-1}\rangle$ *p*1	1	$\langle xy^{-1}, xa^3\rangle$ *p*2	5	$\langle x^4, xy^{-1}\rangle$ *p*1	1	$\langle x^4, xy^{-1}\rangle$ *p*1	1
	$m = -n$	$\langle x^4, xy^{-1}, xa^5b\rangle$ *pg*	2	$\langle xy^{-1}, xa^3, a^5y^{-1}bx\rangle$ *p*2*gg*	10	$\langle x^4, xy^{-1}, xa^5b\rangle$ *pg*	2	$\langle x^4, xy^{-1}, axab\rangle$ *pg*	7

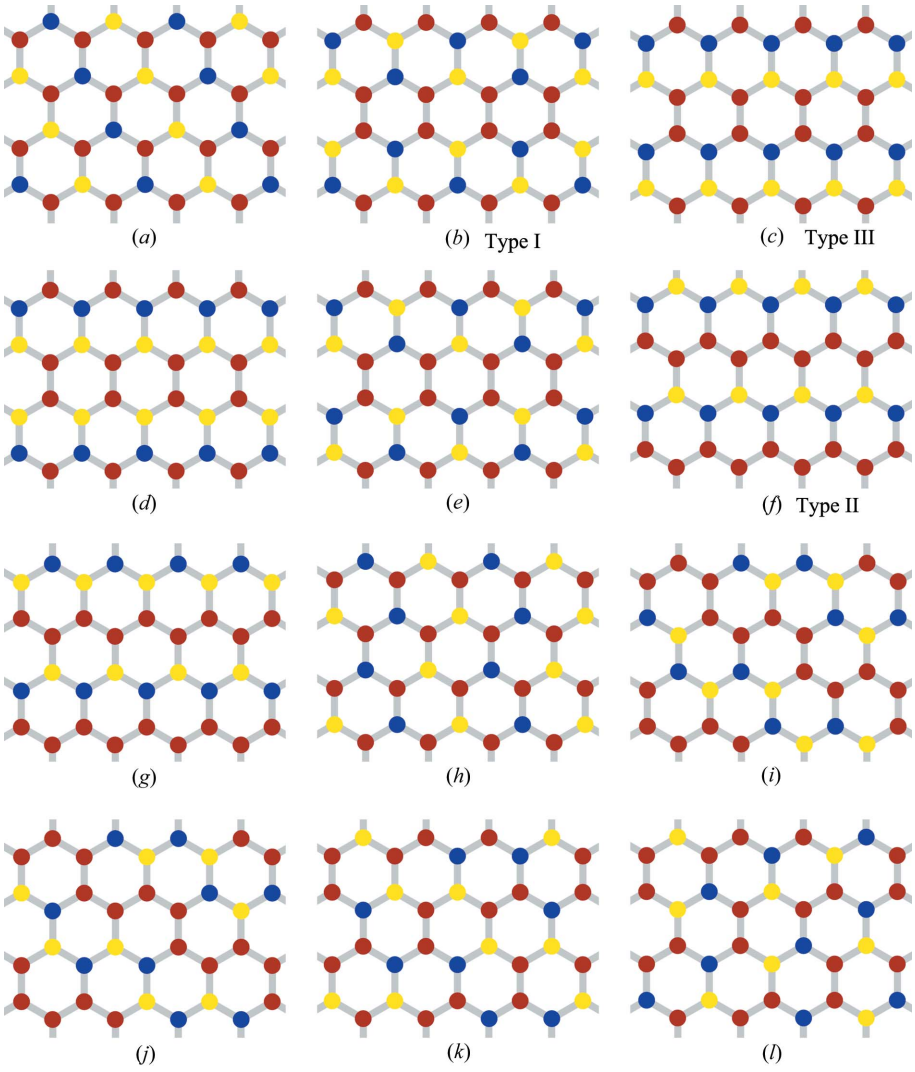

Figure 8
Vertex 3-colorings of the hexagonal tiling that give rise to BC_2N nanotubes. Colorings corresponding to type I, II and III BC_2N nanotubes are labeled. (*a*) $K = \langle x^2, y, ab\rangle \cong pm$, (*b*) $K = \langle x^2, y^2, a^3, b\rangle \cong c2mm$, (*c*) $K = \langle x, y^2, a^3b\rangle \cong pm$, (*d*) $K = \langle x, y^4, a^3, b\rangle \cong p2mm$, (*e*) $K = \langle x^2, xy^2, xa^3, a^3b\rangle \cong p2mg$, (*f*) $K = \langle x, y^2, a^3b\rangle \cong pm$, (*g*) $K = \langle x, y^4, ya^3, a^3b\rangle \cong p2mg$, (*h*) $K = \langle x^2, y^4, ya^3b\rangle \cong pg$, (*i*) $K = \langle x^4, xy^{-1}, xa^5b\rangle \cong pg$, (*j*) $K = \langle xy^{-1}, xa^3, a^5y^{-1}bx\rangle \cong p2gg$, (*k*) $K = \langle x^4, xy^{-1}, xa^5b\rangle \cong pg$, (*l*) $K = \langle x^4, xy^{-1}, axab\rangle \cong pg$.

nanotube given in Fig. 10(*b*). This nanotube points to a possible structural analog of the [4, 0] TUC_4C_8 nanotube (Fig. 9*b*) consisting of three kinds of atoms that appear in the ratio of 1:2:1. We obtain $N_K(L) = K$ and the symmetry group K^* of the nanotube belongs to line group family 6.

7.1. Commensurate and incommensurate nanotubes

Nanotubes that arise by rolling up an isogonal tiling may result in commensurate and incommensurate structures. A nanotube is said to be *commensurate* if the infinite cyclic group of its corresponding line group symmetry structure contains translations along the z axis. Otherwise, the nanotube is said to be *incommensurate*.

In our work, the commensurability of a given nanotube is determined by finding a translation in $N_G(L)$ or $N_K(L)$ (when $\mathbb{S}$ is colored) that is perpendicular to the translation l that generates L. Recall from Table 2 that such a translation in $N_G(L)$ or $N_K(L)$ gives rise to a respective translation in G^* or K^* along the z axis.

An incommensurate nanotube has a symmetry group belonging to either line group family 1 or 5 (Damnjanović *et al.*, 2007; Damnjanović & Milošević, 2010). This is due to the fact that for each of the remaining 11 line group families, a suitable power p of its infinite cyclic group generator results in a translation (not necessarily the minimal one) in the line group. For line group families 2, 3,

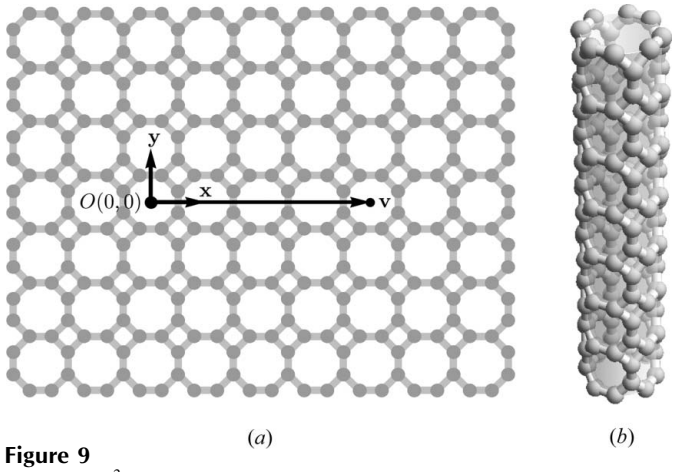

Figure 9
(*a*) The $4 \cdot 8^2$ tiling together with the translation vectors **x**, **y** and the chiral vector $\mathbf{v} = 4\mathbf{x}$. (*b*) The [4, 0] TUC_4C_8 nanotube obtained by rolling up the $4 \cdot 8^2$ tiling in (*a*) along the chiral vector **v**.

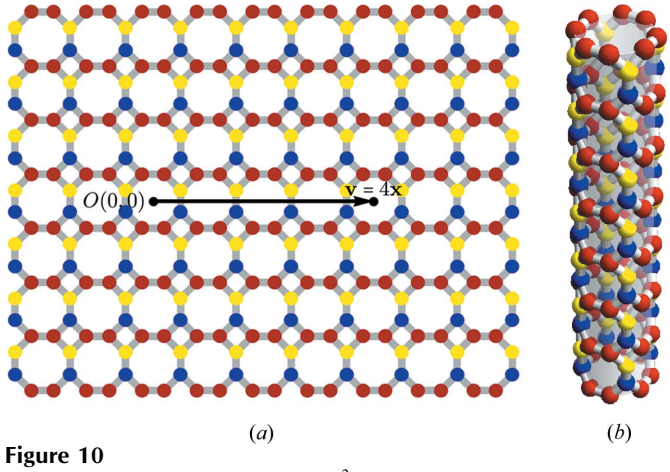

Figure 10
(*a*) A vertex coloring of the $4 \cdot 8^2$ tiling using three colors. (*b*) A 3-coloring of the [4, 0] TUC_4C_8 nanotube suggesting a structural analog made up of three kinds of atoms that appear in the ratio 1:2:1.

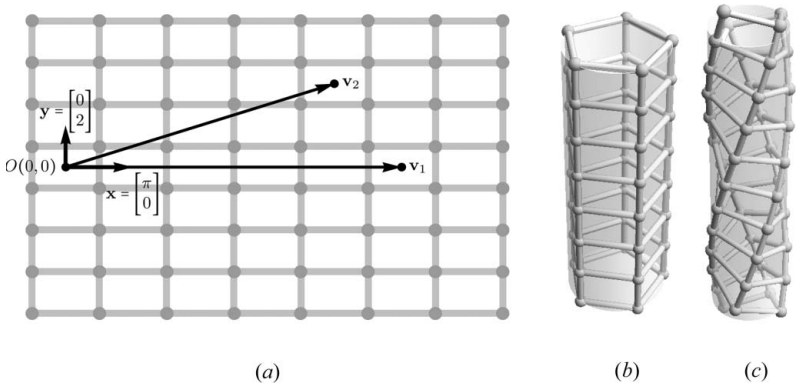

Figure 11
(*a*) The rectangular tiling with translation vectors **x** and **y** as given in equation (1). (*b*) A commensurate nanotube obtained by rolling up the rectangular tiling in (*a*) along the chiral vector $\mathbf{v}_1 = 5\mathbf{x}$. (*c*) An incommensurate nanotube obtained by rolling up the rectangular tiling in (*a*) along the chiral vector $\mathbf{v}_2 = 4\mathbf{x} + 2\mathbf{y}$.

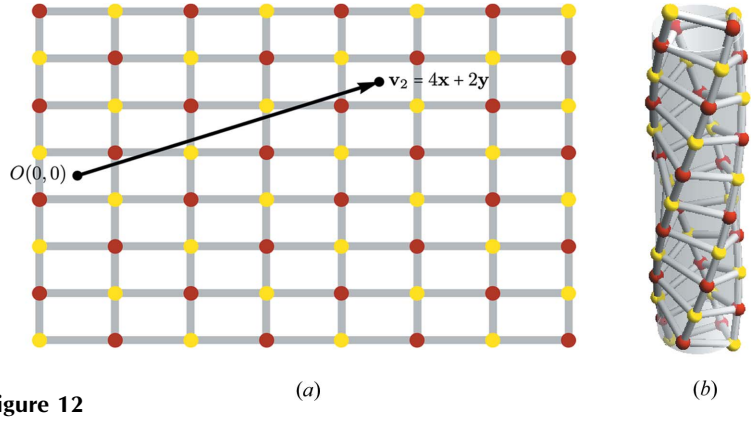

Figure 12
(*a*) A vertex 2-coloring of the rectangular tiling given in Fig. 11(*a*). (*b*) A 2-coloring of the [4, 2] nanotube in Fig. 11(*c*).

6, 9, 11 with infinite cyclic group generator τ (a translation), we have $p = 1$; for families 7, 10, 12 with infinite cyclic group generator γ (a glide reflection), $p = 2$; and for families 4, 8, 13 with infinite cyclic group generator ζ (a screw rotation with rotation component of order $2d$, where d is the order of the line group's generating rotation), we have $p = 2d$. See Table 3 for details of each line group family's generators. Moreover, Table 3 clarifies that if $N_G(L)$ or $N_K(L)$ is one of the plane crystallographic groups *cm*, *pm*, *c2mm*, *p2mm*, *pg*, *p2mg* and *p2gg*, then we obtain a commensurate nanotube. An incommensurate nanotube may arise if $N_G(L)$ [respectively, $N_K(L)$] is of type *p*1 or *p*2. We remark further that incommensurate nanotubes only occur when $N_G(L)$ or $N_K(L)$ has an underlying parallelogramic (oblique), rectangular or rhombic (centered rectangular) lattice structure. This is because a translation perpendicular to l is always present if the lattice of $N_G(L)$ or $N_K(L)$ is square or hexagonal. Thus, a single-wall carbon nanotube or a TUC_4C_8 nanotube is always commensurate regardless of its chiral vector.

We present in Fig. 11(*a*) a rectangular tiling with symmetry group $G = \langle x, y, a, b \rangle \cong p2mm$ having basis vectors

$$\mathbf{x} = \begin{bmatrix} \pi \\ 0 \end{bmatrix}, \mathbf{y} = \begin{bmatrix} 0 \\ 2 \end{bmatrix}. \quad (1)$$

The group G is generated by the twofold (counterclockwise) rotation a about O, the reflection b about the line through O in the direction of **x**, and the translations x, y. Depending on the chiral vector along which it is rolled, this rectangular tiling gives rise to both commensurate and incommensurate nanotubes.

The nanotube in Fig. 11(*b*) is obtained by rolling the rectangular tiling along the vector $\mathbf{v}_1 = 5\mathbf{x}$. We have $N_G(L) = \langle x, y, a, b \rangle \cong p2mm$. This tells us the nanotube is commensurate with its symmetry group G^* belonging to line group family 11. On the other hand, the nanotube in Fig. 11(*c*) is obtained by rolling the same tiling along the vector $\mathbf{v}_2 = 4\mathbf{x} + 2\mathbf{y}$. Observe that $N_G(L) = \langle x, y, a \rangle \cong p2$ and does not contain a translation perpendicular to x^4y^2. This nanotube is incommensurate and its symmetry group G^* belongs to line group family 5.

As a last example, we present a 2-coloring of the rectangular tiling (Fig. 12*a*) that gives rise to a nanotube (Fig. 12*b*) using the chiral vector $\mathbf{v}_2 = 4\mathbf{x} + 2\mathbf{y}$. The color fixing group is given by $K = \langle x^2, xy, a, yb \rangle \cong c2mm$ and $N_K(L) = \langle x^2, xy, a \rangle \cong p2$. Note that $N_K(L)$ also does not contain a translation perpendicular to x^4y^2. This nanotube is also incommensurate and its symmetry group K^* belongs to line group family 5.

Table 9
Symmetry groups of TUC_4C_8 nanotubes according to chirality.

Nanotubes containing reflectional symmetries are classified as achiral while those without are classified as chiral.

Chirality		$N_G(L)$	$G^* \cong N_G(L)\backslash L$	Line group
Chiral		$\langle x, y, a^2 \rangle \cong p2$	$(C_d \times \mathbb{Z}) \rtimes C_2$ $d = gcd(m, n)$	5
Achiral	$n = 0$	$\langle x, y, b, a^2b \rangle \cong p2mm$	$(C_m \times \mathbb{Z}) \rtimes D_2$	11
	$m = 0$	$\langle x, y, b, a^2b \rangle \cong p2mm$	$(C_n \times \mathbb{Z}) \rtimes D_2$	11
	$m = n$	$\langle x, y, ab, a^3b \rangle \cong c2mm$	$(C_m \times \mathbb{Z}) \rtimes D_2$	13
	$m = -n$	$\langle x, y, ab, a^3b \rangle \cong c2mm$	$(C_m \times \mathbb{Z}) \rtimes D_2$	13

8. Conclusion and outlook

In this work, a method to determine symmetry groups of structural analogs of single-wall carbon nanotubes has been presented. We have characterized the symmetry groups of these nanotubes according to line groups. Our approach is to analyze the symmetry group structure of a k-colored hexagonal tiling of the plane which, when folded along a chiral vector, will result in an orbit space model of a single-wall nanotube consisting of k different atoms. Based on the chirality of the nanotube, particular color fixing symmetries will give rise to cylindrical symmetries that will define the line group symmetry structure of the nanotube.

We have determined that the symmetry group of a nanotube arises from one of the 13 line group families and that the type of symmetry group obtained for a particular type of nanotube varies, depending on the chirality. We have derived the symmetry groups of BN, BC_3, BCN and BC_2N nanotubes.

The color symmetry approach presented here in studying the symmetry groups of nanotubes in a two-dimensional setting suggests a convenient and accessible way of analyzing the line group symmetries. It also facilitates the characterization of the possible line group structures alongside the various arrangements of atoms that exist and are theoretically possible on a nanotube, made possible by a coloring framework (De Las Peñas *et al.*, 2006, 2011) applied to construct vertex colorings of the hexagonal tiling.

The method presented to characterize symmetry groups of carbon nanotubes and their structural analogs may also be applied to nanotubes with other symmetries by studying their corresponding isogonal tilings on the plane. These nanotubes include the incommensurate ones, which may arise from tilings with underlying parallelogramic (oblique), rectangular or rhombic (centered rectangular) lattice structure, depending on the tiling's color fixing symmetries.

A possible next step in the study is to determine the symmetry groups of double-wall and multi-wall nanotubes using a similar method.

Another potential problem that can be addressed for future work is to characterize the symmetry group structures of nanotori and investigate other types of symmetric arrangements of various atoms theoretically possible on a torus.

MLANDLP and AMB would like to acknowledge funding support from the National Research Council of the Philippines (NRCP). MLANDLP is also grateful to Ken-ichi Shinoda and Yasushi Gomi for helpful discussions and to the Mathematics Department of Sophia University, Tokyo Japan, where part of the research was carried out. MLL thanks the Office of the Dean of the School of Science and Engineering (SOSE), Ateneo de Manila University, for research support.

References

Alon, O. E. (2001). *Phys. Rev. B*, **64**, 1–4.
Arezoomand, M. & Taeri, B. (2009). *J. Geom. Phys.* **59**, 1168–1174.
Azevedo, S. & de Paiva, R. (2006). *Europhys. Lett.* **75**, 126–132.
Baake, M. (1997). *J. Phys. A Math. Gen.* **30**, 2687–2698.
Barros, E. B., Jorio, A., Samsonidze, G. G., Capaz, R. B., Souza Filho, A. G., Mendes Filho, J., Dresselhaus, G. & Dresselhaus, M. S. (2006). *Phys. Rep.* **431**, 261–302.
Bugarin, E. P. C., De Las Peñas, M. L. A. N., Evidente, I. F., Felix, R. P. & Frettloeh, D. (2008). *Z. Kristallogr.* **223**, 785–790.
Bugarin, E. P., De las Peñas, M. L. A. N. & Frettlöh, D. (2013). *Geom. Dedicata*, **162**, 271–282.
Chopra, N. G., Luyken, R. J., Cherrey, K., Crespi, V. H., Cohen, M. L., Louie, S. G. & Zettl, A. (1995). *Science*, **269**, 966–967.
Cotfas, N. (2006). *J. Phys. A Math. Gen.* **39**, 9755–9765.
Damnjanović, M. & Milošević, I. (2010). *Line Groups in Physics*, *Lecture Notes in Physics*, Vol. 801. Berlin, Heidelberg: Springer-Verlag.
Damnjanović, M., Milošević, I., Vuković, T. & Sredanović, R. (1999). *Phys. Rev. B*, **60**, 2728–2739.
Damnjanović, M., Nikolić, B. & Milošević, I. (2007). *Phys. Rev. B*, **75**, 1–4.
Damnjanović, M., Vuković, T., Milošević, I. & Nikolić, B. (2001). *Acta Cryst.* A**57**, 304–310.
De Las Peñas, M. L. A. N., Felix, R. P., Gozo, B. R. & Laigo, G. R. (2011). *Philos. Mag.* **91**, 2700–2708.
De Las Peñas, M. L. A. N., Felix, R. P. & Laigo, G. R. (2006). *Z. Kristallogr.* **221**, 665–672.
Dresselhaus, M., Dresselhaus, G. & Saito, R. (1995). *Carbon*, **33**, 883–891.
Endo, M., Iijima, S. & Dresselhaus, M. S. (1996). *Carbon Nanotubes*. Oxford: Elsevier Science.
Evarestov, R. A. & Panin, A. I. (2012). *Acta Cryst.* A**68**, 582–588.
Evarestov, R. A., Zhukovskii, Y. F., Bandura, A. V. & Piskunov, S. (2010). *J. Phys. Chem. C*, **114**, 21061–21069.
Grünbaum, B. & Shephard, G. C. (1978). *Trans. Am. Math. Soc.* **242**, 335–353.
Harker, D. (1978). *Proc. Natl Acad. Sci. USA*, **75**, 5751–5754.
Heydari, A. & Taeri, B. (2009). *Eur. J. Combin.* **30**, 1134–1141.
Iijima, S. & Ichihashi, T. (1993). *Nature (London)*, **363**, 603–605.
Kopský, V. & Litvin, D. B. (2002). Editors. *International Tables for Crystallography*, Vol. E, *Subperiodic Groups*, 1st ed., p. 75. Dordrecht: Kluwer Academic Publishers.
Lifshitz, R. (1997). *Rev. Mod. Phys.* **69**, 1181–1218.
Liu, A., Wentzcovitch, R. & Cohen, M. (1989). *Phys. Rev. B*, **39**, 1760–1765.
Loyola, M. L., De Las Peñas, M. L. A. N. & Basilio, A. M. (2012). *Z. Kristallogr.* **227**, 672–680.
Milošević, I. & Damnjanović, M. (2006). *J. Phys. Condens. Matter*, **18**, 8139–8147.
Miyamoto, Y., Rubio, A., Louie, S. & Cohen, M. (1994). *Phys. Rev. B*, **50**, 18360–18366.
Pan, H., Feng, Y. P. & Lin, J. (2009). *Nanoscale Res. Lett.* **4**, 498–502.
Rapanut, T. A. (1988). *Subgroups, Conjugate Subgroups and n-Color Groups of the Seventeen Plane Crystallographic Groups*. Diliman, Quezon City: University of the Philippines.
Ratcliffe, J. G. (2006). *Foundations of Hyperbolic Manifolds*. New York: Springer.
Reich, S., Thomsen, C. & Maultzsch, J. (2004). *Carbon Nanotubes: Basic Concepts and Physical Properties*. Weinheim: Wiley-VCH Verlag GmbH and Co. KGaA.
Saito, R., Dresselhaus, G. & Dresselhaus, M. S. (1998). *Physical Properties of Carbon Nanotubes*. Singapore: Imperial College Press.
Scheffer, M. & Lück, R. (1999). *J. Non-Cryst. Solids*, **250–252**, 815–819.
Schwarzenberger, R. L. E. (1984). *Bull. London Math. Soc.* **16**, 209–216.
Senechal, M. (1979). *Discrete Appl. Math.* **1**, 51–73.
Senechal, M. (1985). *J. Math. Phys.* **26**, 219.
Senechal, M. (1988*a*). *Comput. Math. Appl.* **16**, 545–553.
Senechal, M. (1988*b*). *Discrete Comput. Geom.* **3**, 55–72.
The GAP Group (2008). *GAP – Groups, Algorithms and Programming*, Version 4.4.12. http://www.gap-system.org.
Wang, Q., Chen, L. & Annett, J. (1996). *Phys. Rev. B*, **54**, 2271–2275.
Wolfram Research (2011). *Mathematica Version 8.0 for Microsoft Windows (32-bit)*. http://www.wolfram.com.
Yap, Y. K. (2009). Editor. *B–C–N Nanotubes and Related Nanostructures*. New York: Springer.